ELSEVIER

Ceramics International 31 (2005) 47–52

CERAMICS INTERNATIONAL

www.elsevier.com/locate/ceramint

ETS-synthesized Hi-Nicalon fiber–SiC matrix composite

Wen Yang [a,*], Hiroshi Araki [a], Akira Kohyama [b], Hiroshi Suzuki [a], Tetsuji Noda [a]

[a] *National Institute for Materials Science, 1-2-1 Sengen, Tsukuba 305-0047, Japan*
[b] *Institute of Advanced Energy, Kyoto University, CREST-ACE, Kyoto 611-0011, Japan*

Received 18 December 2003; received in revised form 6 February 2004; accepted 8 March 2004
Available online 26 June 2004

Abstract

Tough ceramic matrix composites, such as SiC/SiC, require a compliant reinforcement/matrix interface coating. The deposition of desired interface coatings on small diameter fibers in SiC/SiC composites is a substantial challenge and costly. A new carbon-rich source gas, ethyltrichlorosilane (ETS), was used to fabric SiC/SiC composite with eight harness satin-woven Hi-Nicalon fabric cloth as reinforcement by the chemical vapor infiltration (CVI) process. A graphite fiber/matrix interlayer was spontaneously formed in the material from the ETS during the CVI matrix densification process, resulting in the composite having a sound interfacial shear stress of 86 MPa. The composite showed a high proportional limit stress of 450 ± 65 MPa and an ultimate flexural strength of 567 ± 75 MPa, coupled with ductile fracture behavior. This study indicates that the costly interfacial coating process might be omitted when ETS is used as source gas for SiC/SiC composite.

Keywords: B. Composite; C. Mechanical properties; D. SiC; Chemical vapor infiltration; Ethyltrichlorosilane

1. Introduction

There has been a strong interest in ceramic matrix composites (CMC) for a variety of high-temperature, high-stress applications in aerospace, hot engine and energy conversion [1–4] because the fracture tolerance of monolithic ceramics can be readily improved by the incorporation of reinforcements fibers, whiskers, and/or particles. The reinforcement/matrix interphase plays a critical role against catastrophic failure for the CMC, especially for continuous fiber reinforced ceramic matrix composites (CFCC). In a CFCC, a transverse matrix crack can be deflected with energy dissipation occurring via several mechanisms as addressed by Besmann et al. [5]: debonding at the fiber/matrix interface, crack deflection, crack bridging by the fibers, fiber sliding, and eventual fiber fracture. These energy–dissipating mechanisms provide for improved apparent fracture toughness and result in a non-catastrophic mode of failure. Obviously, the performance of these mechanisms, and thus the performance of the materials, is closely dependent on the fiber/matrix interfacial shear/sliding strength. A weaker fiber/matrix bonding is prone to crack deflection at the interface while, in order to take advantages of the high strength of the composite fiber reinforcement, the interface must be strong enough for effective load transfer between the fiber and the matrix. Fortunately, this interfacial shear/sliding strength can be adjusted to the required range through the deposition of a compliant fiber/matrix interfacial coating layer(s) [6–9].

A compliant interlayer is necessary for tough SiC/SiC composites. Carbon remains the most effective interphase material [10,11]. However, the deposition of desired interface coatings on small diameter fibers has proved to be a substantial challenge for a variety of processes including solution, sol–gel, and chemical vapor deposition [5].

In this study, a new carbon-rich source gas, ETS ($C_2H_5SiCl_3$), was used rather than the more widely used gas, methyltrichlorosilane (MTS, CH_3SiCl_3) that contains equal carbon and silicon atoms, to fabricate a SiC/SiC composite with automatic graphite interfacial layer formation. The interlayer structures, interfacial shear strength (ISS) and mechanical properties of the material under three-point bending were investigated.

* Corresponding author. Tel.: +81-298-59-2739; fax: +81-298-59-2701.
E-mail address: yang.wen@nims.go.jp (W. Yang).

0272-8842/$30.00 © 2004 Elsevier Ltd and Techna S.r.l. All rights reserved.
doi:10.1016/j.ceramint.2004.03.033

2. Experimental

2.1. Composite process

Eight harness satin-woven as-received Hi-Nicalon fiber clothes (Nippon Carbon, Japan) were used as the reinforcement. The fibrous preform was prepared with eight layers of the fiber cloth in 0–90° stacking and compressed by a set of graphite fixtures to keep a fiber volume fraction of ~40%. The size of the preform was 40 mm in diameter and 2.0 mm in thickness.

The composite was fabricated using a conventional isothermal-CVI system [12], which contains a vertical hot zone. The preform was located in the hot zone within a graphite tube, as shown schematically in Fig. 1. ETS, which was carried by hydrogen through a typical bubble system at constant hydrogen flow rate 1000 sccm and a volume ratio of ETS to hydrogen 0.1, was introduced into the furnace from the bottom of the preform. Thermal decomposition of ETS and SiC matrix deposition would occur in the preform during the CVI process. The process temperature and total pressure were 1000 °C and 14.7 kPa. And the densification process continued for 20 h.

2.2. Single fiber pushout test

Single fiber pushout tests were carried out to extract the ISS using a load controlled micro-indentation testing system with a Berkovich type diamond pyramidal indenter. The maximum load of the indenter is 0.88 N. Detailed experimental procedure can be found elsewhere [8]. The ISS was defined as:

$$\mathrm{ISS} = \frac{F}{(\pi D t)} \quad (1)$$

where F is the onset load for fiber pushout to occur. D and t are the fiber diameter and specimen thickness, respectively.

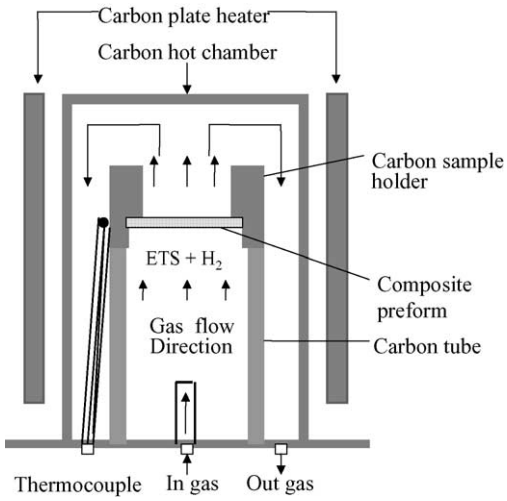

Fig. 1. Schematic configuration of the hot chamber and gas flowing of the CVI process.

The pushout specimen was cut from the composite with one of the fiber bundles perpendicular to the cut surfaces, and was carefully ground and polished at both surfaces with diamond paste to reduce the thickness to ~150 μm. The final polish grain size was 1 μm. Totally 22 single fibers perpendicular to the polished surface were pushed out through the thickness of the specimen to extract the ISS.

2.3. Three-point bending test

Bending bars were prepared from the composite. The bars were cut parallel to one of the fiber bundle directions of the fabric cloth using a diamond wheel and both the tensile and compression surfaces were carefully ground using diamond slurry. The final dimension of the bars was 30 mm (L) × 4.0 mm (W) × 1.5 mm (T). Three-point bending tests (with a support span of 18 mm) were conducted on three specimens at room temperature to derive the strength of the composite. The crosshead speed was 0.0083 mm/s.

2.4. Microstructure characterization

The cross-section and pore distribution in the fabricated composite were inspected by means of a scanning electron microscopy (SEM, JSM-6100). The microstructure and the fiber/matrix interlayer were examined by means of a high-resolution transmission electron microscopy (HRTEM, JEOL JEM-2010F) as well as the SEM. The fracture surfaces, with interfacial debonding and fiber pullouts, were examined by the SEM.

3. Results and discussion

3.1. Microstructure and interface layer in the composite

The composite showed a density (from the mass and volume of the composite) of 2.42 mg/m^3. Fig. 2a shows the SEM image of the cross-section of the composite, in which relatively large pores (several tens to over 100 μm in length) are evidency. These pores generally locate at the intersections or between the 0 and 90° fiber bundles. Due to the stain-woven texture of the reinforcement, simple stacking in 0–90° of the fabric layers often results in large pores in the preform at the intersections or between the fiber bundles. During the CVI process, SiC matrix did not sufficiently filled in theses areas, resulting in those relatively large pores in Fig. 2a. More appropriate arrangement between the fabric layers and/or improved efficiency of the CVI matrix densification is necessary for composite with higher density. Nevertheless, the higher magnification SEM image (Fig. 2b) shows that the intra-fiber bundle areas were rather well filled by the matrix phase. The total porosity of the composite is ~17%.

Fig. 3 shows the TEM image of the microstructures of the fiber, matrix and interlayer of the composite as well as re-

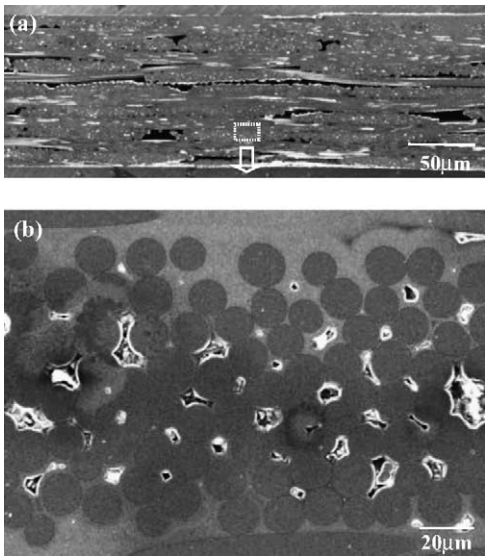

Fig. 2. SEM images of the cross-section (a) and intra-fiber bundle pores (b) of the composite.

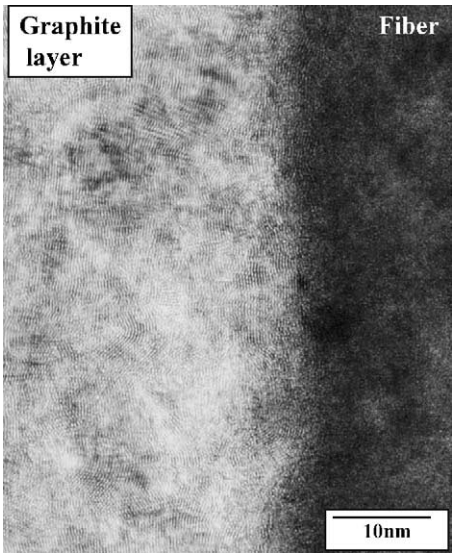

Fig. 4. HRTEM image showing the granular graphite structure of the interlayer.

lated selected area electron diffraction (SAD) patterns. The fiber has a poly-crystal β-SiC structure, as is well known. The TEM image and the SAD of the matrix indicate a highly-crystal β-SiC structure with the growing direction radially away from the fiber. Between the fiber and the matrix, the image clearly shows the existence of an interfacial layer. The SAD taken from this area indicates a graphite structure, which is confirmed by the HRTEM image (Fig. 4). During the CVI process, following basic chemical reactions occurred [13].

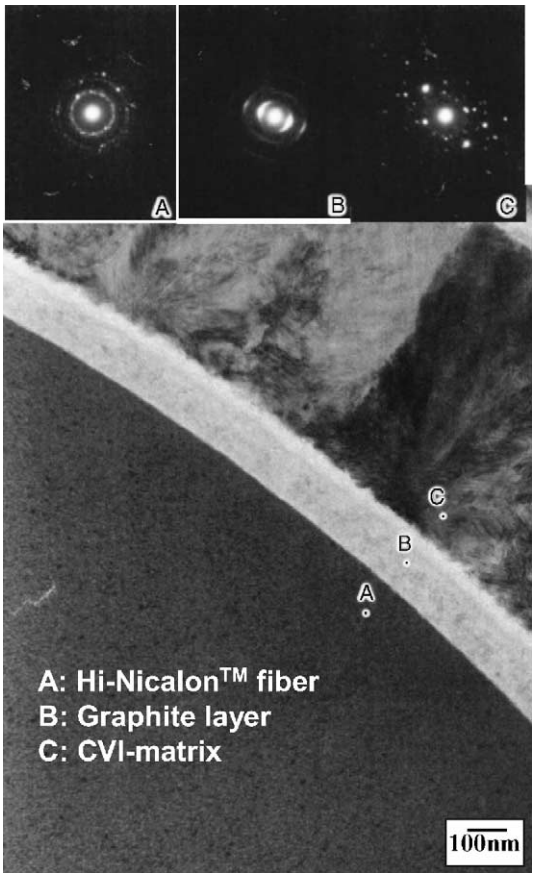

Fig. 3. TEM image and SAD patterns of the fiber, the matrix, and the interlayer.

$$C_2H_5SiCl_3 + H_2 = SiC + 3HCl + CH_4$$

$$CH_4 = C + 2H_2$$

Extra carbon was produced from above second reactions. As known from the experimental section, the Hi-Nicalon fibers are as-received ones. No fiber coating was pre-deposited before the CVI process. Therefore, it is believed that the graphite layer was formed during the CVI process owing to the extra carbon from above reactions. The thickness of the graphite layer is ~180 nm. The detailed mechanism of the formation of the graphite interlayer currently remains unclear. However, the thickness of this graphite layer showed some process conditions dependence, especially at the initial stage of the CVI. As mentioned before, compliant interlayer(s) is necessary for tough SiC/SiC composites, this study indicates that ETS might be a good source material for the fabrication of CVI-SiC/SiC composites with automatic formation of graphite interlayer, provided further studies on the control the thickness of this layer.

3.2. Fracture behavior and flexural strength

Fig. 5 shows the load–displacement curves, which displays several common features among the three specimens: an initial linear region, reflecting the elastic response of the materials, followed by a non-linear domain of deformation, due to the matrix cracking, interfacial debonding and fiber

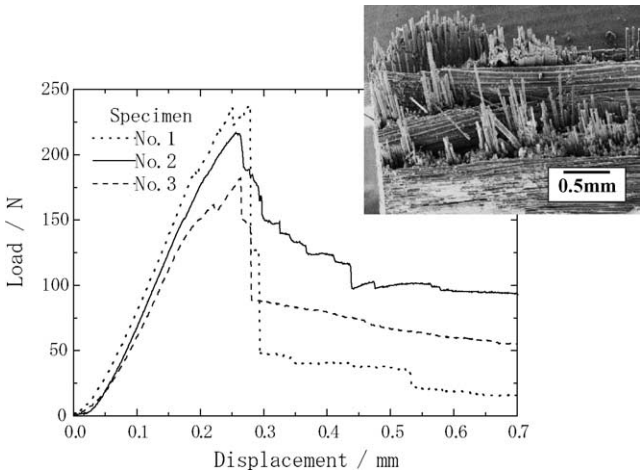

Fig. 5. Load–displacement curves.

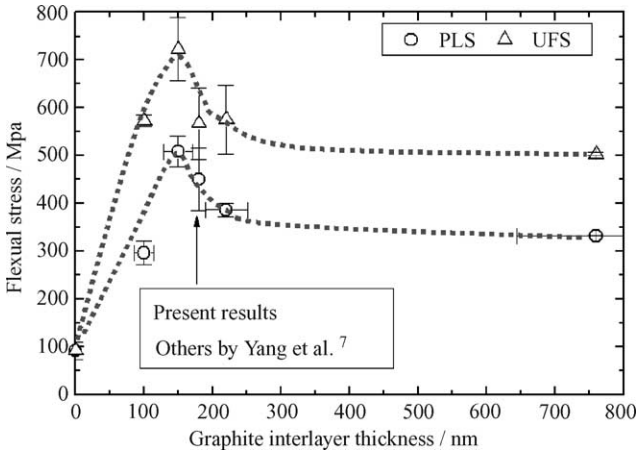

Fig. 6. Graphite interlayer thickness dependence of the PLS and UFS of various Hi-Nicalon/SiC composites.

sliding, and failures of the fibers. A significant fraction of fibers failed after the specimens achieved their load maximums, beyond which the specimens showed certain levels of down-hill side load till large displacement. The fracture surfaces showed interfacial debonding and sound fiber pullouts fracture behaviors, as typically shown in the inserted SEM image in Fig. 5.

The proportional limit stress (PLS) and ultimate flexural strength (UFS) of the composite were derived from the load–displacement curves and are listed in Table 1. The UFS was determined according to simple beam theory as:

$$\mathrm{UFS} = \frac{3}{2}\frac{PL}{WT^2} \quad (2)$$

where P is the flexural load. L is the load-supporting span (18 mm). W and T are the width and thickness of the specimen, respectively. The PLS is the stress corresponding to a 0.01% offset strain [14]. The average PLS and UFS are 450 ± 65 MPa and 567 ± 75 MPa, respectively.

3.3. Effect of the graphite interlayer

Tough ceramic matrix composites require a compliant reinforcement/matrix interlayer. Initially, there was little concern with regard to the thickness of the graphite layer in a SiC/SiC composite. It was assumed that the fibers were long and the entanglements in the bundles would allow the tow to act like ropes thus providing sufficient reinforcement to carry the load at the onset of matrix load [15]. Further studies on the composites revealed that the thickness of this layer is also important in determining the performance of the materials [6,7]. A recent efforts on a systematic study on the effects of graphite interlayer thickness on the flexural properties of 2D CVI-Hi-Nicalon/SiC composites has been reported [7]. Those composites were fabricated using MTS. The graphite interlayers of different thickness in the composites were deposited using an isothermal CVI coating process prior to the fabrication of the composites. Including the strengths of present composite in their results to relate the PLS and UFS to the graphite layer thickness resulted in Fig. 6, which indicates a just-fit PLS but a slightly lower UFS of the present composite according to the strength-graphite thickness trends. However, considering the relatively large error bars, such a difference in the UFS is not significant. This indicates that SiC/SiC composites from ETS would not suffer from significant change/loss in strength but with the advantage of spontaneous graphite interlayer formation.

Table 1
Density, interfacial structures, and mechanical properties of the composites

Density (mg/m^3)	Interlayer (nm)	Flexural strength			ISS (MPa)
		Specimen	PLS (MPa)	UFS (MPa)	
		No. 1	521	637	
		No. 2	433	577	
		No. 3	395	487	
2.42	180 (graphite)	Average	450 ± 65	567 ± 75	86 ± 19

3.4. Interfacial shear strength and its effects on PLS

The composite exhibited incatastrophic failure behavior (Fig. 5) with interfacial debonding and sound fiber pullouts at the fracture surface, indicating a reasonable interfacial bonding strength. To confirm this, the ISS was investigated using single fiber pushout tests, and the result is given in Table 1. The average ISS is 86±19 MPa, which is far smaller than that of a Hi-Nicalon/SiC composite (505 ± 91 MPa) from MTS, in which no interlayer was deposited [8]. The high ISS of latter composite caused a brittle failure of the material with rather low and same value of PLS and UFS, 91 ± 18 MPa. While, the ductile fracture behavior of present ETS-composite with markedly improved strengths, 450 ± 65 MPa and 567 ± 75 MPa for PLS and UFS, respectively,

is because of the moderate ISS, which is owing to the spontaneous formed graphite interlayer.

Inghels and Lamon [16] have developed a theoretical approach to predict the strength of unidirectional SiC/SiC composites upon flexural loading from the properties of the fiber, matrix and the interface. Yang et al. [8] applied the theory to calculate the PLS of plain-woven Hi-Nicalon fabric cloth reinforced CVI-SiC/SiC composites with a simple assumption that the 90° bundles could be regarded as 'matrix', and an empirical coefficient, K(=0.66), defined from a comparison between the model prediction and experimental results for their composite system:

$$\mathrm{PLS} = K\sigma_{\mathrm{PLS}}^{\mathrm{Th}} \tag{3}$$

where $\sigma_{\mathrm{PLS}}^{\mathrm{Th}}$ is the theoretical prediction giving by:

$$\sigma_{\mathrm{PLS}}^{\mathrm{Th}} = E_{\mathrm{c}}\left(\frac{12\gamma_{\mathrm{m}}E_{\mathrm{f}}V_{\mathrm{f}}'^{2}\mathrm{ISS}}{E_{\mathrm{c}}E_{\mathrm{m}}^{2}(1-V_{\mathrm{p}}-V_{\mathrm{f}}')r_{\mathrm{f}}}\right)^{1/3} \times\left(\frac{E_{\mathrm{c}}+E_{\mathrm{f}}V_{\mathrm{f}}'}{2E_{\mathrm{f}}V_{\mathrm{f}}'}\right)\left(\frac{4E_{\mathrm{f}}V_{\mathrm{f}}'}{3E_{\mathrm{c}}+E_{\mathrm{f}}V_{\mathrm{f}}'}\right)^{1/3} \tag{4}$$

where γ_{m} is the surface energy of CVD-SiC, which was given as 25 J/m^2 [16]. E_{m} and E_{f} are the Young's modulus of the matrix and the fiber, 400 and 270 GPa for typical CVI-SiC matrix and the Hi-Nicalon fiber, respectively. V_{f}' and V_{p} are the volume fractions of the 0° bundle fibers and porosity, which are 20 and 17% for the present composite, respectively. E_{c} is the composite modulus determined from the law of mixture:

$$E_{\mathrm{c}} = E_{\mathrm{f}}V_{\mathrm{f}}' + E_{\mathrm{m}}(1-V_{\mathrm{p}}-V_{\mathrm{f}}') \tag{5}$$

Using Eqs. (3)–(5), the PLS of present composite was calculated to be 389 MPa. The calculated value is slightly lower than the experimental observation (Table 1). The model, as well as the empirical coefficient $K = 0.66$, was derived from a family of SiC/SiC composites with plain-woven reinforcements. Further modification of the model is necessary for an improved estimation of the strength of SiC/SiC composite from ETS with eight harness satin-woven cloth reinforcement.

4. Conclusions

A new source gas, ETS, was used for fabricating a SiC/SiC composite with eight harness satin-woven Hi-Nicalon cloth as the reinforcement. A spontaneous graphite interlayer formation was observed in the composite during the CVI matrix densification, which was attributed to the extra carbon from the thermal decomposition of the ETS. This graphite interlayer adjusted the interfacial shear strength to a reasonable range, and therefore, yielded the composite with ductile fracture behavior and high flexural strength of 450 ± 65 MPa and 567 ± 75 MPa for PLS and UFS, respectively. This study indicates that ETS might be an alternative source material (in stead of MTS) for the fabrication of CVI-SiC/SiC composites with advantage of spontaneously formed graphite interlayer (the additional interlayer deposition process might become unnecessary in this case). However, further studied on the detailed mechanism of the spontaneously formation of the graphite interlayer is necessary for the controlling the thickness of the layer.

Acknowledgements

This work is supported by the CREST, Japan Science and Technology Corporation and conducted at the National Institute for Materials Science. A part of this study was financially supported by the Budget for Nuclear Research of the Ministry of Education, Culture, Sports, Science and Technology, based on the screening and counseling by the Atomic Energy Commission.

References

[1] G.N. Morscher, J.D. Cawley, Intermediate temperature strength degradation in SiC/SiC composites, J. Eur. Ceram. Soc. 22 (14/15) (2002) 2777–2787.
[2] T. Noda, H. Araki, F. Abe, M. Okada, Microstructure and mechanical properties of FCVI carbon fiber/SiC composites, J. Nucl. Mater. 191–194 (1992) 539–543.
[3] D. Brewer, HSR/EPM combustor materials development program, Mater. Sci. Eng. A261 (1999) 284–291.
[4] K.M. Prewo, J.J. Brennan, Silicon carbide fiber reinforced glass-ceramic matrix composites exhibiting high strength and toughness, J. Mater. Sci. 17 (1982) 2371–2383.
[5] T.M. Besmann, D.P. Stinton, E.R. Kupp, S. Shanmugham, P.K. Liaw, Fiber–matrix interfaces in ceramic composites, J. Mater. Res. Soc. Symp. Proc. 458 (1997) 147–159.
[6] R.A. Lowden, Fiber coatings and the mechanical properties of a fiber-reinforced ceramic composite, Ceram. Trans. 19 (1991) 619–663.
[7] W. Yang, H. Araki, T. Noda, J.Y. Park, Y. Katoh, T. Hinoki, J. Yu, A. Kohyama, Hi-Nicalon^{TM} fiber-reinforced CVI-SiC matrix composites: I effects of PyC and PyC–SiC multilayers on the fracture behaviors and flexural properties, Mater. Trans. 43 (10) (2002) 2568–2573.
[8] W. Yang, H. Araki, A. Kohyama, Y. Katoh, Q. Hu, H. Suzuki, T. Noda, Hi-Nicalon^{TM} fiber-reinforced CVI-SiC matrix composites: II interfacial shear strength and its effects on the flexural properties, Mater. Trans. 43 (10) (2002) 2574–2577.
[9] R. Naslain, The concept of layered interlayers in SiC/SiC, Ceram. Trans. 58 (1995) 23–29.
[10] F. Rebillat, J. Lamon, R. Naslain, E. Lare-Curzio, M.K. Ferber, T.M. Besmann, Interfacial bond strength in SiC/C/SiC composite materials, as studied by single-fiber pushout tests, J. Am. Ceram. Soc. 81 (4) (1998) 965–978.
[11] C. Droillard, J. Lamon, X. Bourrat, Strong interface in CMCs a condition for efficient multilayered interlayers, Mater. Res. Soc. Symp. Proc. 365 (1995) 371–376.
[12] W. Yang, Development of CVI process and property evaluation of CVI-SiC/SiC composites. Ph.D. thesis, Institute of Advanced Energy, Kyoto University, 2002.

[13] A.I. Kingon, L.J. Lutz, P. Liaw, R.F. Davis, Thermodynamic calculations for the chemical vapor deposition of silicon carbide, J. Am. Ceram. Soc. 66 (8) (1983) 558–566.
[14] ASTM C 1341-97, Standard test method for flexural properties of continuous fiber-reinforced advanced ceramic composites, 2000, pp. 509–526.
[15] R.W. Rice, Mechanisms of toughening in ceramic matrix composites, Ceram. Eng. Sci. Proc. 2 (7/8) (1981) 661–682.
[16] E. Inghels, J. Lamon, An approach to the mechanical behavior of SiC/SiC and C/SiC ceramic matrix composites, part II theoretical approach, J. Mater. Sci. 26 (1991) 5411–5419.